

# Cusp-shaped structure of a jet observed by *IRIS* and *SDO*

Yuzong Zhang and Jun Zhang

Key Laboratory of Solar Activity, National Astronomical Observatories, Chinese Academy of Sciences, Beijing 100012, China; yuzong@nao.cas.cn; zjun@nao.cas.cn

Received \_\_\_\_\_; accepted \_\_\_\_\_

Not to appear in Nonlearned J., 45.

## ABSTRACT

On 29 August 2014, the trigger and evolution of a cusp-shaped jet were captured in detail at 1330 Å by the *Interface Region Imaging Spectrograph*. At first, two neighboring mini-prominences arose in turn from low solar atmosphere and collided with a loop-like system over them. The collisions between the loop-like system and the mini-prominences lead to the blowout and then a cusp-shaped jet formed with a spire and an arch-base. In the spire, many brightening blobs originating from the junction between the spire and the arch-base, moved upward in a rotating manner and then in a straight line in the late phase of the jet. In the arch-base, dark and bright material simultaneously tracked in a fan-like structure and the majority of the material moved along the fan's threads. At the later phase of the jet's evolution, bidirectional flows emptied the arch-base, while down-flows emptied the spire, thus making the jet entirely vanish. The extremely detailed observations in this study shed new light on how magnetic reconnection alters the inner topological structure of a jet, and provide a beneficial complement for understanding current jet models.

*Subject headings:* Sun: chromosphere — Sun: filaments, prominences

## 1. Introduction

A solar jet is a highly dynamic, transient, and well collimated eruption phenomenon, which is thought to contribute to coronal heating and solar wind acceleration (Brueckner & Bartoe 1983; Pariat et al. 2009; Tian et al. 2014). With the soft X-ray telescope (Tsuneta et al. 1991) on board the *Yohkoh* satellite (Ogawara et al. 1991), Shibata et al. (1992) discovered X-ray jets, forcefully motivating the jet study on observations and related theories. Generally, the family members of jets, including spicule, photospheric jet, H $\alpha$  surge, Ca II H jets, EUV jet, X-ray jet, and macro spicule, can potentially be observed by all spectral lines of present instruments with quite distinct morphology and structure (Pariat et al. 2010), such as standard jets (Shibata et al. 1992; Yokoyama & Shibata 1995), blowout jets (Moore et al. 2010, 2013) and micro-sigmoid jets (Raouafi et al. 2010). In principle, a jet is composed of an arch-base and an elongated spire standing on the arch-base.

With the improvement of the observational capability on the solar atmosphere, more new features on the jet geometry, dynamics, and physical property are unceasingly revealed. For example, the extensive rotating or spinning motions in the spire show an untwisting mechanism (Canfield et al. 1996; Nisticò et al. 2009; Liu et al. 2011b; Shen et al. 2011; Chen et al. 2012; Liu et al. 2014; Cheung et al. 2015; Lee et al. 2015). The upflowing motion along the spire could even reach to a very high speed approximately 800 km s<sup>-1</sup>, which is near the local Alfvén speed and this suggested to possibly contribute to the high-speed solar wind in a coronal hole (Cirtain et al. 2007). Recently, some recurrent helical jets were reported (Cirtain et al. 2007; Pariat et al. 2010; Innes et al. 2011; Tian et al. 2014; Cheung et al. 2015; Chen et al. 2015), and well reproduced by numerical simulations on the oscillatory magnetic reconnection between an emerging field and a pre-existing active region field (Archontis et al. 2010). Moreover, the recurrent jets

with untwisting motions and upflowing at near the local Alfvén speed were reproduced in the numerical experiment by Lee et al. (2015), directly showing that the helical jet is related to the torsional Alfvén wave propagating in the corona. In addition, a jet spire frequently appears whipping-like motion, suggesting a relaxing process of the reconnected magnetic field (Yokoyama & Shibata 1995; Shimojo et al. 2007). From the same case in Shimojo et al. (2007), Zhang & Ji (2014a) first observed the transverse oscillation of the spire. Furthermore, the multi-temperature observations by different instruments prove the jet temperature is not unique, comprising cool and hot components (Zhang et al. 2000; Jiang et al. 2007; Nishizuka et al. 2008). Additionally, with the higher spatial and temporal resolution observations at EUV wavebands, some jets have been found to have micro-CME (coronal mass ejection) like shape (Nisticò et al. 2009; Shen et al. 2012), which hint a scale-invariant eruptive phenomenon of the Sun (Raouafi et al. 2016).

Based on the key mechanism of magnetic reconnection for impulsively releasing energy, two main models on jet are very popular at present. One is the standard model, which is proposed and numerically simulated in two dimensions (2D), and 3D (Heyvaerts et al. 1977; Shibata et al. 1992; Yokoyama & Shibata 1995; Yokoyama & Shibata 1996; Shimojo et al. 1996; Nishizuka et al. 2008; Pariat et al. 2009). In this model the closed magnetic arch emerges into the ambient unipolar field and then reconnection occurs between the unipolar field and one branch of the arch with an opposite polarity to the unipolar field. The other is the blowout model (Moore et al. 2010, 2013) with two magnetic reconnection processes. The first magnetic reconnection, which is similar to that in the standard model, occurs between the emerging magnetic arch and the ambient unipolar field. Then a filament with a large amount of pent-up free energy by shear (or twist) dominates the second magnetic reconnection (Liu et al. 2011a,b; Moreno-Insertis & Galsgaard 2013; Hong et al. 2014; Lee et al. 2015). Recently, Sterling et al. (2015) suggested that all of the jets in the coronal hole essentially come from mini-filament eruptions. According to the latest

review (Raouafi et al. 2016), the standard jets are intensively collimated, usually form an inverse-Y shape with a narrow spire, and seldom rotate. However, the blow-out jets strongly rotate, and possess a relatively broad spire. As suggested by Pariat et al. (2010), a jet process is always dominated by a synthetic role from magnetic geometrical characteristics of the jet source, such as size, flux distribution, null point position, and asymmetry. Many observations find that jets could appear with similar morphology and outflow, but might possess distinctive magnetic structures in the low coronal source region (Nisticò et al. 2009; Zhang et al. 2012).

In total, a large number of observations and theoretical models basically describe and explain the morphology, dynamical and physical properties of the jets. However, for the limitation of observational capability, there is no appreciable resolution to distinctly resolve the motions of the plasma blobs (Zhang & Ji 2014b) and related variation of magnetic topological structure inside a jet. Fortunately, benefitting from the extremely high spatial and temporal resolution in special wavelength observations by the *Interface Region Imaging Spectrograph* (IRIS; De Pontieu et al. 2014) and all ultraviolet (UV) and extremely ultraviolet (EUV) wavelengths of the Atmosphere Imaging Assembly (AIA; Lemen et al. 2012) aboard the *Solar Dynamics Observatory* (SDO; Pesnell et al. 2012), a cusp-shaped structure jet was captured with unprecedented detailed observations. The formation and evolution processes of the jet, including the motions of the blobs and topological variation of its skeleton, are described in Sec. 2. Section 3 contains discussion and conclusions.

## 2. Observations

### 2.1. Data

From 05:51 UT to 06:39 UT on 29 August 2014, *IRIS* narrow-band slit-jaw images (SJIs) (see Fig. 1) in the 1330 Å channel captured a cusp-shaped jet located at N08W90 (Solar-X: 935'' and Solar-Y: 185'') in detail. The field of view (FOV) of each SJI 1330 was 119''×119'', but total SJIs 1330 covering a larger Solar-Y range of 133'' by scanning the solar surface from north to south with an eight-step round and a 2'' step length. The jet was located exactly at the northernmost region of the larger FOV; therefore, a data gap in the north fraction of the jet with a width range of 2''–14'' was unavoidable while the FOV of the SJIs 1330 left the northernmost region. However, the main jet process was still successfully recorded. As a complement, all the UV and EUV data observed by *SDO/AIA* were adopted to display the different temperature components of the jet. The time cadence and the spatial resolution of the SJIs are 9.6 s and 0.166'' per pixel, respectively, while those of the images observed by the *SDO/AIA* are 12 s and 0.6'' per pixel, respectively. Furthermore, to ease reading, all of the images were rotated 90° counterclockwise, i.e., the left and right represent the original north and south, respectively. Finally, a smaller FOV, with a Solar-X size of 60'' (from 991'' to 931'') and a Solar-Y size of 38'' (from 144'' to 182'') was cut to merely focus the jet.

### 2.2. Formation and evolution of the cusp-shaped jet from *IRIS* observations

At 05:51:04 UT on 29 August 2014 a closed-loop-like structure (hereafter, “loop”; and marked “L1” in Fig. 1) appeared in the *IRIS* SJI 1330 and then slowly ascended with a speed of approximately 15 km s<sup>-1</sup>. Five minutes later, a mini-prominence (see “P1” in Fig. 1) with an uneven brightness structure appeared under the loop and ascended with a higher

speed of approximately  $65 \text{ km s}^{-1}$ . Affected by the newly appearing mini-prominence, the loop accelerated to a much higher speed of approximately  $50 \text{ km s}^{-1}$ . One minute after its appearance, P1 expanded violently and collided with L1 (see Figs. 1C and D). In the following 2 min, L1 covered and prevented P1 from freely expanding and erupting, resulting in both of them moving up together at a speed of about  $60 \text{ km s}^{-1}$ . Simultaneously, many small cusp-shaped structures appeared at the common apex of L1 and P1 (e.g., the “Cusp 1” in panel E of Fig. 1). These small cusp-shaped structures contributed a tunnel for plasma blobs flowing out from the erupted mini-prominence. Then these small cusp-shaped structures developed and merged into one cusp-shaped structure with an outstanding spire at the apex of its arch-base. Later, another pair of mini-prominence (P2) and loop-like system (L2) also collided and formed another cusp-shaped structure (see Figs. 1G-I). Finally, the above two cusp-shaped structures combined into a complete jet structure with a notable cusp-shaped structure composed of a spire and an arch-base. The width of the arch-base is mostly the same as that of L1 when L1 collided with P1. Therefore, the jet in this event consists of two sets of similarly cusp-shaped structures with some distinction in scale. Totally, it merely took 9 minutes for the formation of the jet since the first loop appeared.

Subsequently, a huge number of bright plasma blobs (e.g., shown by the diamonds in Fig. 2A) appeared and traced in detail the topological evolution of the jet. These plasma blobs first moved up from the bottom of the left leg of the arch-base. As they arrived at the junction of the spire and the arch-base, they started to bifurcate and formed a bidirectional flow. The solid blue arrows in Fig. 2A show one branch of the bidirectional flow moving up along the spire, while the dashed blue arrow denotes the other branch moving down along the right leg of the arch-base. For the plasma continuously discharging from the left leg of the arch-base, the original thick left leg degraded to a clear skeleton, which is composed of three thin legs (see Fig. 2B). Then bright plasma blobs (see Figs. 2D-E) were ceaselessly

flowing up/down along these thin legs, subsequently these legs became thinner. Some details are illustrated in Figs 3A-D, e.g., a couple of brightening blobs appeared at about 06:03:03 UT, and then immediately separated. One blob (marked by solid circles) moved downwards with the speed of approximately  $64 \text{ km s}^{-1}$ , meanwhile the other one (marked by asterisks) was elongated and ascended also along the thin leg. Additionally, the size of an identified smallest blob in this jet reaches to about  $0.8''$  (see the blob denoted by the long green arrow passing through Figs. 2D and E). These thinner legs became extreme thin and then completely broke at approximately 06:06:53 UT (see Fig. 2F) resulting in the arch-base disappearance, hence only the spire of the jet remained.

As shown in Figs. 2G-H and more details in Figs. 3E-H, continually brightening processes led to the appearance of up/down-flows near the elbow of the remaining bending spire. The up-flows were apparently accelerated, as well as the down-flows pushed powerfully down the spire elbow. At about 06:09:26 UT, a violent “explosion” occurred at the left edge of the elbow, resulting in some plasma blobs promptly moving upwards with a speed of approximately  $163 \text{ km s}^{-1}$ , while others moving down. Later, the productivity of the brightening processes gradually slowed down. After 06:20:46 UT, while the brightening processes finally ceased in the jet, an amount of plasma began to directly flow back to the solar surface along the spire. Then the spire grew fainter, and completely vanished at about 06:39:26 UT.

### 2.3. Complementary *SDO/AIA* observations of the jet

To compensate the missing data of the jet in the *IRIS* SJIs 1330, we adopted a total of nine wavelength images in the UV and EUV captured by the *SDO/AIA* as complementary observations. We found that the basic configuration and evolution process of the jet observed by both solar satellites are quite similar. However, for distinct temperature

responses at different wavelengths, there are outstanding observational distinctions in detail. Regarding the observations of the first pair of the loop and the mini-prominence by AIA, only a fraction of L1 and most of P1 could be captured at 1600 Å. No loop could be seen, but dark P1 appeared at 193 Å. A part of L1 and P1 could be observed at 335 Å. Figures 4E-I display both L1 and P1 as a dark region at 304 Å. During the evolution stage of the jet, much dark matter was observed at 304 Å to escape from P1 and almost float around the whole jet. In addition, the bright and dark matter traced the fan-like skeleton of the arch-base.

At 171 Å P1 displayed as a dark feature before colliding with L1. After the collision, several bright points appeared in dark P1. Gradually, the arch-base structure became more and more distinctive amidst the ambient dark mini-prominence material. With most of the dark material moving around the spire, the remainder was finally heated as the bright ingredients of the arch-base. During both the formation and evolution processes of the cusp-shaped jet, many mini-bright-points appeared in the left branch of the arch-base. Four bright points and their motion processes are clearly presented in Fig. 5. After the collision between L1 and P1, the first bright point (cf. Figs. 5A and B) appeared, moved up and was elongated into a bright thread-like structure in the formation process of the spire. The first one and the following two bright points (see Figs. 5A-F), spanning both the formation and the evolution processes of the jet, are found outstanding rotation along the spire. However, after the arch-base disappeared for the sudden collapse of the thinner legs mentioned in Fig. 2F, the rotation of the spire slowed down. Therefore, the fourth bright point shown in Figs. 5G and H, just moved along a thread-like structure in the spire without any obvious rotating behavior. Additionally, after the last bundle of light material out-poured up from the elbow of the remaining spire at 06:23:29 UT (cf. Fig. 2I), all of material began to fall down along the spire without any apparent rotation.

### 3. Discussion and conclusions

In this study, from the observations by *IRIS* SJIs 1330 and *SDO/AIA* in all the UV and EUV wavelengths with unprecedented spatial and temporal resolution, we are offered a chance to learn about the formation of a cusp-shaped jet and the dynamics of the material in the jet. In the previous literatures, it is seldom reported that a cusp-shaped jet with a broad spire and an arch-base forms by the collisions between loop-like system and mini-prominences. A lot of brightening blobs moved upward along the spire in a rotating manner, and some material moved downward along the arch-base. Finally, the bidirectional flows emptied the spire and the arch-base, thus making the jet vanish.

Moore et al. (2010, 2013) proposed dichotomy of solar coronal jets, i.e. standard jets and blowout jets. Their observational samples show a cool component in all blowout jets and in a minority of standard jets, outstanding lateral expansion in the former but none in the latter, and obvious axial twist in both classes of jets. Recently, Sterling et al. (2015, 2016) suggested that both standard and blowout jets are related to the filament eruptions but in different explosion intensity. In this event, the collision between the loop-like system and the mini-prominence leads to the blowout and then the jet forms. The cool component, lateral expansion and obvious axial rotation of the spire of the jet are all observed. These properties are consistent with the scenarios described by them. However, besides of the mini-prominence eruptions, the loop-like system also takes part in the jet formation. The loop-like system keeps the mini-prominence from free eruption and forms a fine arch-base together with the mini-prominence. Therefore, this event basically fits into the scenarios described by Moore et al. (2010, 2013) and Sterling et al. (2015, 2016) with new features, which are mainly benefited from the extremely high observational resolution by *IRIS*. Totally, the jet appears all of the typical observational features of the blowout jet (e.g., an outstanding rotation, a relatively broad spire and a mini-filament eruption) reviewed by the

latest literature (Raouafi et al. 2016) and completely fits with the class of blowout jet.

The closed loop-like system in this case is easily reminiscent of another two jets reported by Liu et al. (2009) and Liu et al. (2014). In particular, a distinct loop is also observed in Liu et al. (2009). In the jets studied by them, the spires of the jets show evidently helical motions, which denote the untwisting magnetic field lines and are usually supposed to be a characteristic of a blowout jet. Additionally, both of their spires appear interesting transverse motions or wriggling perpendicular to the jet axis. However, the jet described in this paper shows that the spire gradually formed by a series of small cusp structures which merge and grow without outstanding transverse motions. Nevertheless, thanks to the high spatial resolution and suitable observational angle, the detailed formation and evolution processes of the arch base and the plasma blob motions are clearly captured, which might shed new light into the physical mechanism in the interior of a jet.

Among these small-scale brightening plasma blobs, their smallest size even reaches to  $0.8''$ , which is consistent with that of the observations in Ca II H by the Solar Optical Telescope (SOT, Tsuneta et al. 2008; Singh et al. 2012) aboard *Hinode* (Kosugi et al. 2007), but much smaller than that in observations by *SDO/AIA* (Zhang & Ji 2014b). These brightening blobs trace the bidirectional flows forming at the junction of the arch-base and spire, the variation of the rotation velocity of the spire, and the detailed evolution in the fan-like branches of the arch-base. Once all of the brightening blobs disappear in the late phase of the jet, an enormous amount of material immediately returns back to the solar surface, resulting in the final disappearance of the jet.

Significantly, we observed many brightening plasma blobs (see Figs. 2D-E) and bidirectional flow (Innes et al. 1997) traced by these blobs (see Figs. 3A-D) in the interior of the jet. These observational evidence suggests that there exist plenty of magnetic reconnection processes. In theory, according to the VAL-C model (Vernazza et al. 1981;

Fontenla et al. 1993) for the upper chromosphere, the magnetic Reynolds number is quite outstanding on the order of  $10^6$ , which easily leads to the magnetic island appearance during the magnetic reconnection process (Bhattacharjee et al. 2009). Moreover, in the recent numerical experiments on the jet process (Yang et al. 2013; Ni et al. 2015), it is found that comparing to their plasma environment, the magnetic islands always possess relatively higher temperature and density, so appear more bright. Therefore, these brightening blobs, which could be used to trace the bidirectional flows, are extremely possibly magnetic islands occurring in the process of magnetic reconnection for the tearing-mode instability (Furth et al. 1963; Kliem et al. 2000; Asai et al. 2004; Lin et al. 2005; Ni et al. 2012; Kumar & Cho 2013; Zhang & Ji 2014b). This hints that there are complex and ubiquitous magnetic reconnections of different scales in the entire jet process to heat and transfer the material, as well as alter the magnetic topological structure.

*IRIS* is a NASA Small Explorer mission developed and operated by LMSAL with mission operations executed at NASA ARC and major contributions to downlink communications funded by the NSC (Norway). *SDO* data and images are courtesy of NASA/*SDO* and the AIA and HMI science teams. The work is supported by the National Natural Science Foundation of China (11533008, 11303049, 11673034, and 11673035), the Strategic Priority Research Program-The Emergence of Cosmological Structures of Chinese Academy of Sciences (No. XDB09000000).

## REFERENCES

- Archontis, V., Tsinganos, K. & Gontikakis, C. 2010, *A&A*, 512, 2
- Asai, A., Yokoyama, T., Shimojo, M., & Shibata, K. 2004, *ApJ*, 605, L77
- Bhattacharjee, A., Huang, Y.-M., Yang, H. & Rogers, B. 2009, *Phys. Plasmas*, 16, 112102
- Brueckner, G. E., & Bartoe, J.-D. F. 1983, *ApJ*, 272, 329
- Canfield, R. C., Reardon, K. P., Leka, K. D., et al. 1996, *ApJ*, 464, 1016
- Chandrashekar, K., Bemporad, A., Banerjee, D. , Gupta, G. R. & Teriaca, L. 2014, *A&A*, 561, 104
- Chen, H.-D., Zhang, J., & Ma, S.-L. 2012, *Research in Astronomy and Astrophysics*, 12, 573
- Chen, J., Su, J., Yin, Z., et al. 2015, *ApJ*, 815, 71
- Cheung, M. C. M., De Pontieu, B., Tarbell, T. D., et al. 2015, *ApJ*, 801, 83
- Cirtain, J. W., Golub, L., Lundquist, L., et al. 2007, *Science*, 318, 1580
- De Pontieu, B., Title, A. M., Lemen, J. R., et al. 2014, *Sol. Phys.*, 289, 2733
- Fontenla, J. M., Avrett, E. H., & Loeser, R. 1993, *ApJ*, 406, 319
- Furth, H. P., Killeen, J., & Rosenbluth, M. N. 1963, *Physics of Fluids*, 6, 459
- Guo, J., Liu, Y., Zhang, H., et al. 2010, *ApJ*, 711, 1057
- Heyvaerts, J., Priest, E. R., & Rust, D. M. 1977, *ApJ*, 216, 123
- Hong, J., Jiang, Y., Yang, J., et al. 2014, *ApJ*, 796, 73

- Innes, D. E., Cameron, R. H., & Solanki, S. K. 2011, *A&A*, 531, L13
- Innes, D. E., Inhester, B., Axford, W. I., & Wilhelm, K. 1997, *Nature*, 386, 811
- Jiang, Y. C., Chen, H. D., Li, K. J., Shen, Y. D., & Yang, L. H. 2007, *A&A*, 469, 331
- Kliem, B., Karlicky, M., & Benz, A. O. 2000, *A&A*, 360, 715
- Kosugi, T., Matsuzaki, K., Sakao, T., et al. 2007, *Sol. Phys.*, 243, 3
- Kumar, P., & Cho, K.-S. 2013, *A&A*, 557, A115
- Lee, E. J., Archontis, V., & Hood, A. W. 2015, *ApJ*, 798, L10
- Lemen, J. R., Title, A. M., Akin, D. J., et al. 2012, *Sol. Phys.*, 275, 17
- Lin, J., Ko, Y.-K., Sui, L., et al. 2005, *ApJ*, 622, 1251
- Liu, C., Deng, N., Liu, R., et al. 2011a, *ApJ*, 735, L18
- Liu, J., Wang, Y., Liu, R., et al. 2014, *ApJ*, 782, 94
- Liu, W., Berger, T. E., Title, A. M., Tarbell, T. D., & Low, B. C. 2011b, *ApJ*, 728, 103
- Liu, W., Berger, T. E., Title, A. M., & Tarbell, T. D. 2009, *ApJ*, 707, 37
- Moore, R. L., Cirtain, J. W., Sterling, A. C., & Falconer, D. A. 2010, *ApJ*, 720, 757
- Moore, R. L., Sterling, A. C., Falconer, D. A., & Robe, D. 2013, *ApJ*, 769, 134
- Moreno-Insertis, F., & Galsgaard, K. 2013, *ApJ*, 771, 20
- Ni, L., Roussev, I. I., Lin, J., & Ziegler, U. 2012, *ApJ*, 758, 20
- Ni, L., Kliem, B., Lin, J. & Wu, N. 2015, *ApJ*, 799, 79
- Nishizuka, N., Shimizu, M., Nakamura, T., et al. 2008, *ApJ*, 683, L83

- Nisticò, G., Bothmer, V., Patsourakos, S., & Zimbardo, G. 2009, *Sol. Phys.*, 259, 87
- Ogawara, Y., Takano, T., Kato, T., et al. 1991, *Sol. Phys.*, 136, 1
- Pariat, E., Antiochos, S. K., & DeVore, C. R. 2009, *ApJ*, 691, 61
- Pariat, E., Antiochos, S. K., & DeVore, C. R. 2010, *ApJ*, 714, 1762
- Pesnell, W. D., Thompson, B. J., & Chamberlin, P. C. 2012, *Sol. Phys.*, 275, 3
- Raouafi, N. E., Georgoulis, M. K., Rust, D. M., & Bernasconi, P. N. 2010, *ApJ*, 718, 981
- Raouafi, N. E., Patsourakos, S., Pariat, E. et al. 2016, *SSRV*, tmp, 31
- Shen, Y., Liu, Y., Su, J., & Ibrahim, A. 2011, *ApJ*, L735, 43
- Shen, Y., Liu, Y., Su, J., & Deng, Y. 2012, *ApJ*, 745, 164
- Shibata, K., Ishido, Y., Acton, L. W., et al. 1992, *PASJ*, 44, L173
- Shimojo, M., Hashimoto, S., Shibata, K., et al. 1996, *PASJ*, 48, 123
- Shimojo, M., Narukage, N., Kano, R., et al. 2007, *PASJ*, 59, 745
- Singh, K. A. P., Isobe, H., Nishizuka, N., Nishida, K., & Shibata, K. 2012, *ApJ*, 759, 33
- Sterling, A. C., Moore, R. L., Falconer, D. A., & Adams, M. 2015, *Nature*, 523, 437
- Sterling, A. C., Moore, R. L., Falconer, D. A., Panesar, N. K., Akiyama, S., Yashiro, S., & Gopalswamy, N. 2016, *ApJ*, 821, 100
- Tian, H., DeLuca, E. E., Cranmer, S. R., et al. 2014, *Science*, 346, 1255711
- Tsuneta, S., Acton, L., Bruner, M., et al. 1991, *Sol. Phys.*, 136, 37
- Tsuneta, S., Ichimoto, K., Katsukawa, Y., et al. 2008, *Sol. Phys.*, 249, 167

- Vernazza, J. E., Avrett, E. H., & Loeser, R. 1981, *ApJs*, 45, 635
- Yang, L., He, J., Peter, H., Tu, C., Zhang, L., Feng, X., & Zhang, S. 2013, *ApJ*, 777, 16
- Yokoyama, T., & Shibata, K. 1995, *Nature*, 375, 42
- Yokoyama, T., & Shibata, K. 1996, *PASJ*, 48, 353
- Zhang, J., Wang, J., & Liu, Y. 2000, *A&A*, 361,759
- Zhang, Q. M., Chen, P. F., & Guo, Y. 2012, *ApJ*, 746, 19
- Zhang, Q. M., & Ji, H. S. 2014a, *A&A*, 561, A134
- Zhang, Q. M., & Ji, H. S. 2014b, *A&A*, 567, A11

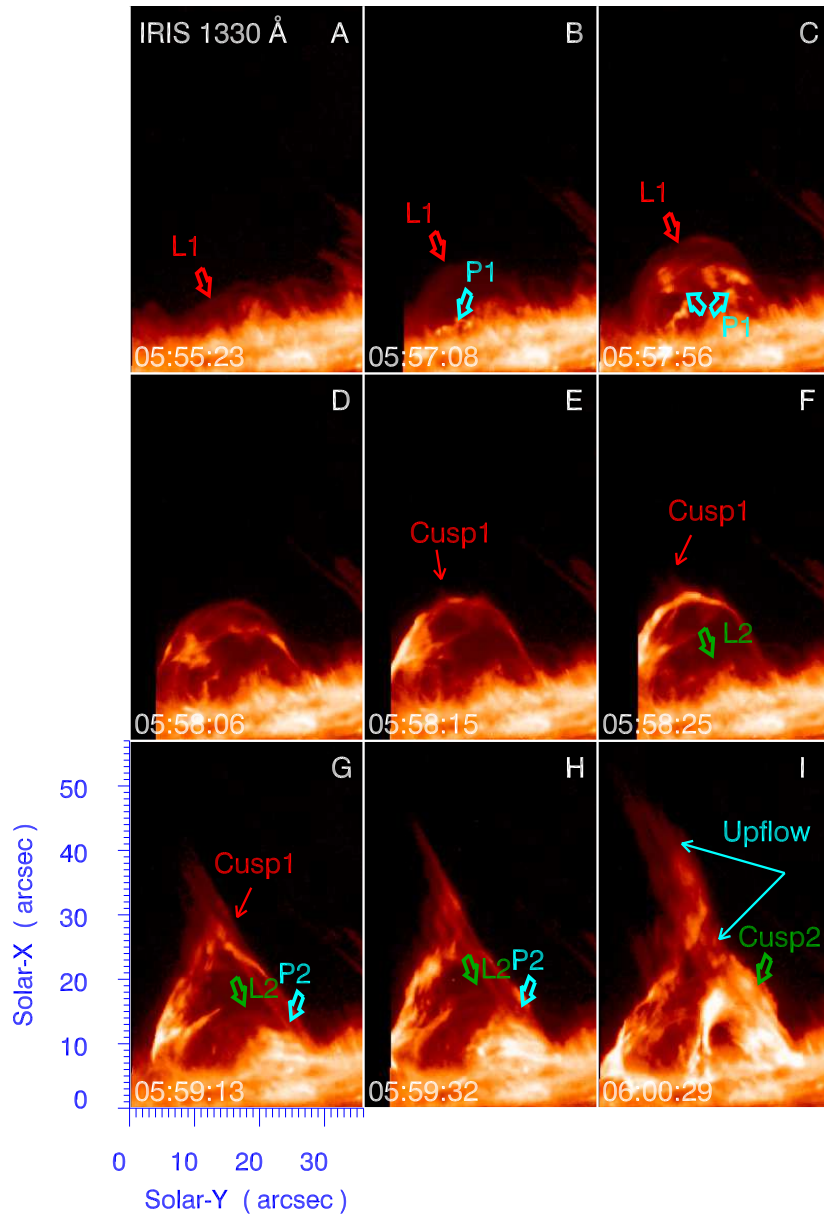


Fig. 1.— Formation process of the cusp-shaped jet observed in the *IRIS* SJIs 1330. “L1” and “L2” denote the first and second closed-loop-like objects; “P1” and “P2” show the first and second mini-prominences. The jet is composed of two cusp-shaped structures “Cusp 1” and “Cusp 2” overlaid on the line of sight. “Upflow” shows the plasma flowing upwards along the spire of the jet.

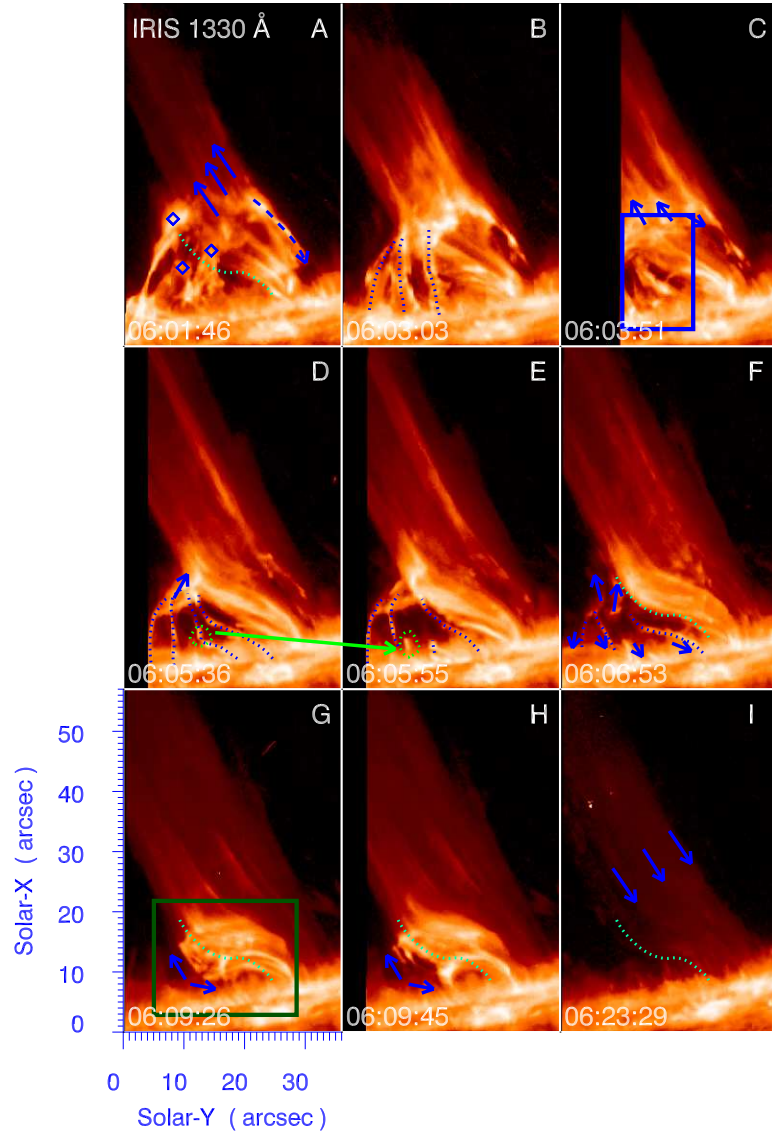


Fig. 2.— Evolution process of the cusp-shaped jet. Diamonds mark the jet plasma blobs. Blue arrows denote the motion directions of the jet plasma at different times. Light green dotted line shows the lower edge of the spire at 06:06:53 UT. Blue dotted lines mark the fine branches of the left leg of the arch-base. Long green arrow links the corresponding plasma in the green dotted circles in panels D and E, respectively. Motions of the plasma in blue and green boxes are described in detail in Fig. 3.

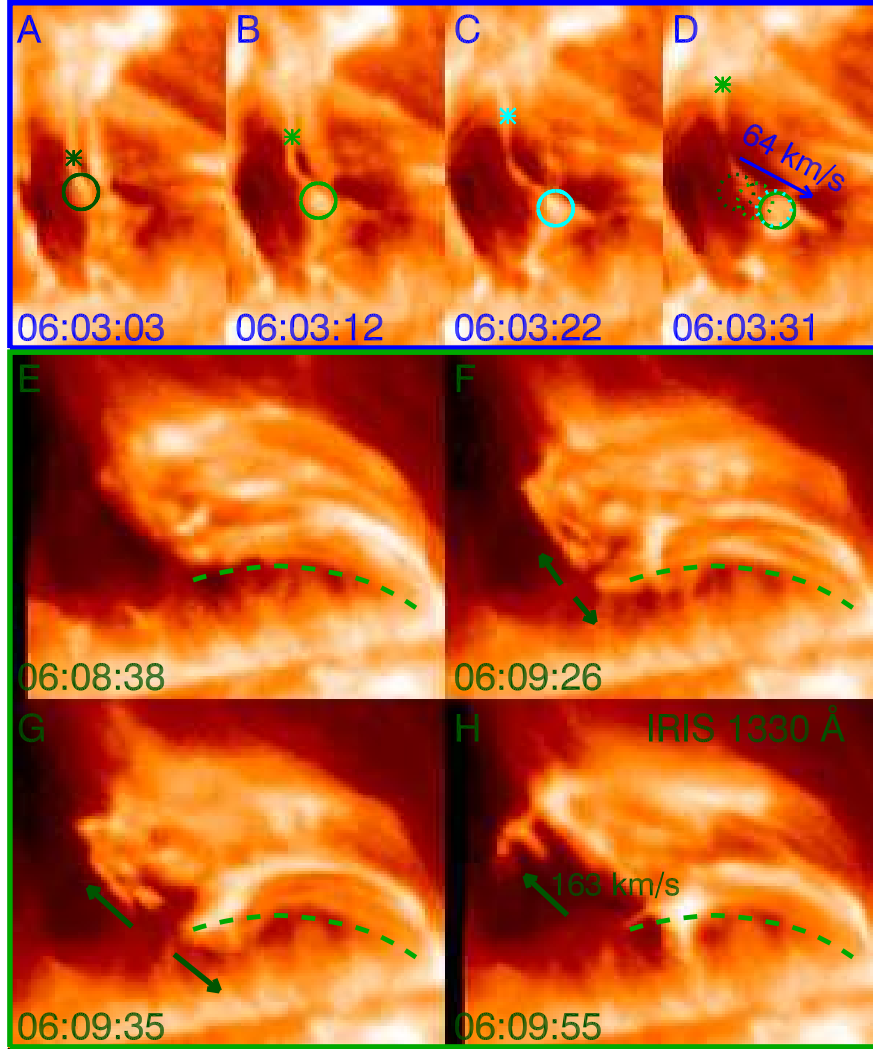


Fig. 3.— Two examples of the plasma motions during the jet evolution process captured by the *IRIS* SJI 1330. Successive images, encircled in blue and green boxes, correspond to those images in blue and green boxes in Fig. 2, respectively. Circles and asterisks in the blue box denote two plasma blobs moving in the opposite directions. Arrows trace the motions of the bright points. Green dashed curve line marks the lower edge of the spire at 06:08:38 UT on 29 August 2014.

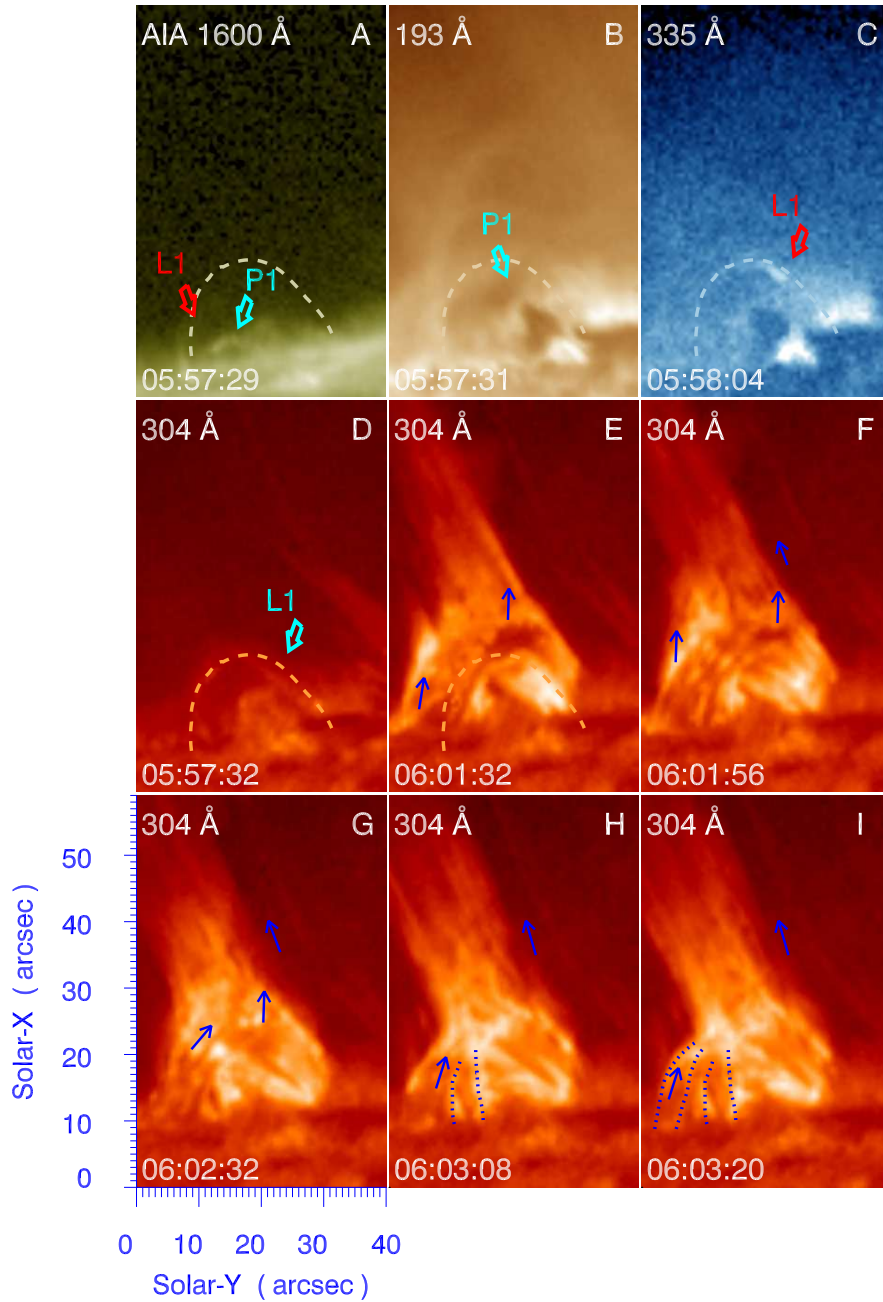


Fig. 4.— Jet observed in four wavelengths by *SDO/AIA*. Dashed line denotes the first closed-loop-like structure in the *IRIS* SJI 1330 at approximately 05:57:56 UT. “L1” and “P1” are the same as those in Fig. 1. Blue dotted lines mark the fine branches of the left leg of the jet. Blue arrows mark the jet legs that are formed from the initial jet.

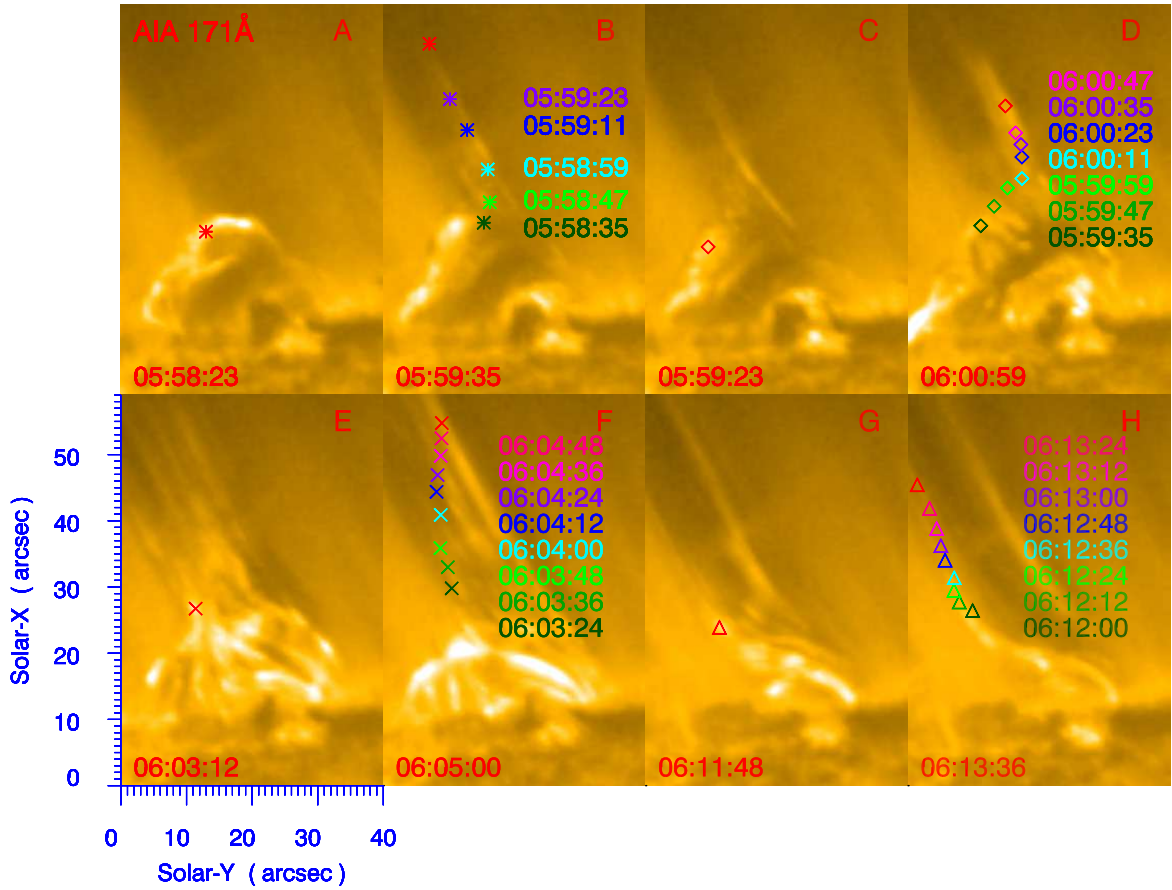


Fig. 5.— Tracking the motions of four brightening points originating from the apex of the arch-base in the successive *SDO*/AIA 171 Å observations. Traces of each brightening point are marked by the same symbols. Time of each position is written in the same color of the corresponding symbol.